Temperature dependent structural changes of graphene layers on 6H-SiC(0001) surfaces

2008 J. Phys.: Condens. Matter 20 225017

(http://iopscience.iop.org/0953-8984/20/22/225017)

J. Phys.: Condens. Matter **20** (2008) 225017 (5pp) doi:10.1088/0953-8984/20/22/225017

Temperature dependent structural changes of graphene layers on 6H-SiC(0001) surfaces

Ki-jeong Kim[1,2], Hangil Lee[1], J-H Choi[2], H-K Lee[3], T-H Kang[1], B Kim[1,3] and Sehun Kim[2]

[1] Beamline Research Division, Pohang Accelerator Laboratory (PAL), POSTECH, Pohang 790-784, Korea
[2] Department of Chemistry and School of Molecular Science (BK21), Korea Advanced Institute of Science and Technology, Daejeon 305-701, Korea
[3] Department of Physics, POSTECH, Pohang, Kyungbuk 790-784, Korea

E-mail: kbs007@postech.ac.kr (B Kim) and sehun-kim@kaist.ac.kr (S Kim)

Received 29 February 2008, in final form 22 April 2008
Published 15 May 2008
Online at stacks.iop.org/JPhysCM/20/225017

Abstract
We investigated the electronic and structural properties of graphene layers grown on a 6H-SiC (Si-terminated) substrate by using core level photoemission spectroscopy (CLPES), low energy electron diffraction (LEED), and near edge x-ray absorption fine structure (NEXAFS). The angle between the plane of the graphene sheet and the SiC substrate was measured by monitoring the variation of the π^* transition in the NEXAFS spectrum with the thickness of the graphene layers. As the thickness of the graphene layers increased, the angle gradually decreased.

(Some figures in this article are in colour only in the electronic version)

1. Introduction

Graphene has been attracting much attention because of its peculiar properties [1]. The unique electrical properties have led many investigators to expect that graphene could be used to overcome the limitations of Si devices. Various studies of graphene have been carried out: theoretical calculations [2], measurements of its physical properties [3–8], its application in electrical devices [9, 10], and methods of synthesizing graphene with reliable properties and its mass production [11]. Yet, it is still difficult to prepare uniform graphene reproducibly because it affects its device applications. Meanwhile, an ultra-thin graphite layer grown on 6H-SiC(0001) by carrying out thermal decomposition has been proposed as a good candidate for use in electrical devices because of its high structural integrity. Moreover, it has been found that this material can be patterned, and intricate submicrometer structures can be constructed by using the standard microelectronics lithography methods, unlike carbon nanotubes which are difficult, if not impossible, to be patterned or formed into any structure.

The structural changes in SiC that result from thermal annealing have been studied extensively. On the basis of their photoemission spectroscopy (PES) results, Johansson *et al* [12]. have suggested that the $(6\sqrt{3}\times 6\sqrt{3})$R30° reconstruction occurs as a result of the depletion of Si around 1150 °C. Graphitization arises only after heating to a temperature higher than that required to produce a $(6\sqrt{3}\times 6\sqrt{3})$R30° diffraction pattern. In contrast, Heer *et al* [6, 7] carried out LEED and STM on SiC after thermal treatment and found that ultra-thin epitaxial graphite ('graphene') films are formed after annealing at 1150 °C. Rotenberg *et al* [13] have measured the band structure of bilayer graphene/SiC with angle resolved ultra-violet spectroscopy (ARUPS) and found that the band structure changes after K doping. They showed that by doping with metal or molecules, the carrier density of graphene is controllable, and so it can be used in atomic devices. Also, much effort has been made to understand the initial stage of the graphene formation [14–22]. In this study, we investigated the basic electronic properties of graphene and the interaction between graphene and the SiC surface by using CLPES, LEED, and NEXAFS.

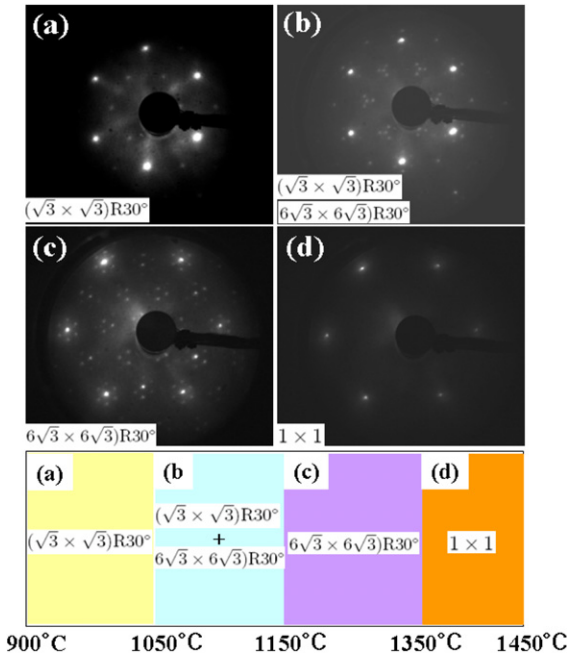

Figure 1. LEED patterns of graphitic layers on SiC after the following heat treatments: (a) at 900 °C (104.9 eV), (b) 1080 °C (98.2 eV), (c) 1150 °C (94.4 eV), and (d) 1400 °C (99.9 eV) for 2 min.

2. Experiment

These experiments were performed in an ultra-high vacuum chamber (base pressure 3×10^{-10} Torr) at the 2B1 photoemission spectroscopy (PES) beamline at the Pohang accelerator laboratory (PAL), which is equipped with an electron analyzer (SES100, Gamma Data Scienta) for PES, a partial electron yield (PEY) detector for NEXAFS, and a low energy electron diffractometer. We used a nitrogen-doped ($N_D \sim 9 \times 10^{17}$ cm^{-3}), Si-terminated 6H-SiC(0001) sample purchased from Cree Research(USA). The annealing temperature was monitored with an infrared pyrometer by assuming an emissivity of 0.90.

After each reconstruction, the Si 2p core level spectra were measured at a photon energy of 130 eV with a total resolution of 200 meV. The C 1s spectra were obtained at a photon energy of 320 eV with a spectral resolution of 350 meV. The photon was impinged on the surface at 45° to the surface normal. The binding energy was calibrated with the Fermi level of a clean Au film. The NEXAFS spectra were measured in the partial electron yield (PEY) detection mode with a retarding voltage of −210 V and an accelerating voltage of 1.8 kV. We were able to obtain molecular bonding information for the top few layers of the multilayer films from the PEY mode NEXAFS spectra by considering probing depths less than 10 Å. The photons had a degree of polarization of about 85%, with an incident photon energy resolution of 350 meV near the carbon K-edge region.

3. Results and discussion

We acquired LEED patterns for graphene on the SiC(0001) surface shown in figure 1 to see the structural changes (surface reconstruction) by varying the annealing temperature. After annealing around 900 °C for 2 min, we deposited Si atoms under an Si flux (1 Å min^{-1}) below 5×10^{-10} Torr, As shown in figure 1(a), we obtained a single phase Si-rich $(\sqrt{3} \times \sqrt{3})$R30° reconstruction. We also obtained reconstructed LEED patterns as we annealed with various annealing temperatures to determine the resulting changes in their reconstructions [15]. At first, annealing was carried out at 1080 °C for 2 min, and we obtained $(\sqrt{3}\times\sqrt{3})$R30° + $(6\sqrt{3}\times 6\sqrt{3})$R30° mixed phase reconstruction patterns, as shown in figure 1(b). By comparing this LEED pattern with that in figure 1(a), we found that the carbon phase is enhanced as we confirmed the presence of the $(6\sqrt{3} \times 6\sqrt{3})$R30° phase in the LEED pattern. However, still no single phase graphene layer was formed. Hence, we increased the annealing temperature up to 1150 °C to track the graphene layer. As shown in figure 1(c), we confirmed that a single phase graphene layer is formed as we see a fair $(6\sqrt{3} \times 6\sqrt{3})$R30° LEED pattern at this annealing temperature. The smallest hexagon is the result of a $(6\sqrt{3} \times 6\sqrt{3})$R30° reconstruction of the interfacial layer, as are the spots lying just inside the graphene pattern. These LEED findings matched well with that of the previous result [23]. Finally, a further annealing at 1400 °C showed that the graphene layer has disappeared and well-ordered graphite is formed with a reconstructed 1×1 LEED pattern. As shown in figure 1(d), the outermost hexagon (spots aligned horizontally) is formed by graphene 1×1 diffraction and the bright six-fold spots aligned vertically in the middle are formed by the SiC 1×1.

Concurrently, we obtained NEXAFS and PES spectra to clarify the change in electronic structures. From the spectral analysis with NEXAFS and PES, we clearly confirm that the variations of electron structures are a function of the annealing temperature.

In figure 2, we utilized complementary information obtained from the carbon K edge of the NEXAFS spectra for (a) 900 °C, SiC substrate, (b) 1080 °C, mixed phase, (c) 1150 °C, single phase graphene layers on SiC(0001), and (d) 1400 °C, thicker graphene layers at various incidence angles. In these spectra, our focus is to determine the flatness and describe the thickness of graphene layer.

Generally, the NEXAFS spectra for graphite are well characterized by a sharp 1s $\rightarrow \pi^*$ peak at 285.5 eV, which is a fingerprint of sp^2 hybridized C atoms, and characterized by the 1s $\rightarrow \sigma^*$ edge at 291.4 eV.

As shown in figures 2(c) and (d) we could clearly see the angle dependence of graphene layers. We could see a SiC NEXAFS spectra measured at an angle of 20° and 90° in figure 2(a), but it did not reveal an angle dependence. Thus, we could assume that this measurement was started from a uniform surface. To determine the average angle between the double bonds of graphene and the SiC(0001) substrate, we used an analytical solution of the NEXAFS intensity problem [25, 26].

The relationship between the photoelectron intensity and the incident photon beam angle can be expressed as follows.

$$I \propto \frac{P}{3}\left\{1 + \frac{1}{2}(3\cos^2\theta - 1)(3\cos^2\alpha - 1)\right\} + \frac{1-P}{2}\sin^2\alpha \quad (1)$$

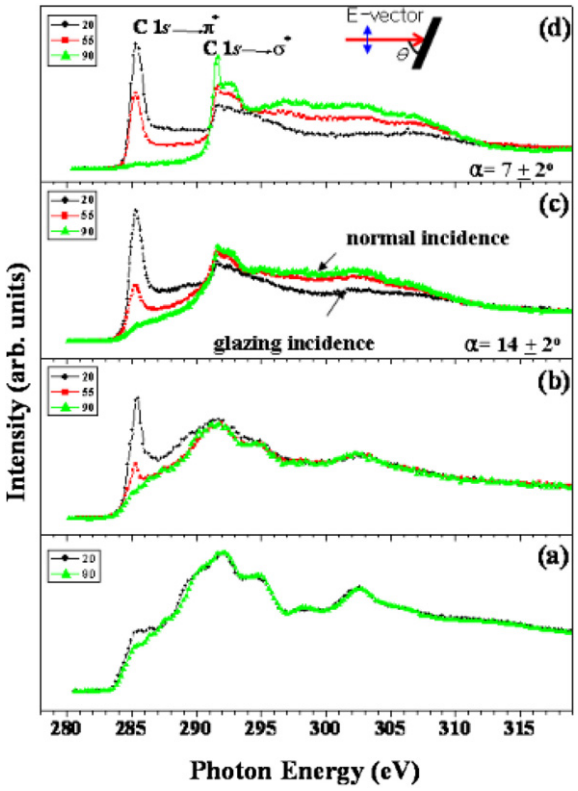

Figure 2. Carbon K-edge NEXAFS spectra 1s $\rightarrow \pi^*$ peak at 285.5 eV, and 1s $\rightarrow \sigma^*$ edge at 291.4 eV measured at various incidence angles of x-rays for the graphene layers on SiC for (a) 900 °C out-gassing, SiC substrate (b) 1080 °C, mixed phase (c) 1150 °C, single phase graphene layers and (d) 1400 °C, thicker graphene layer.

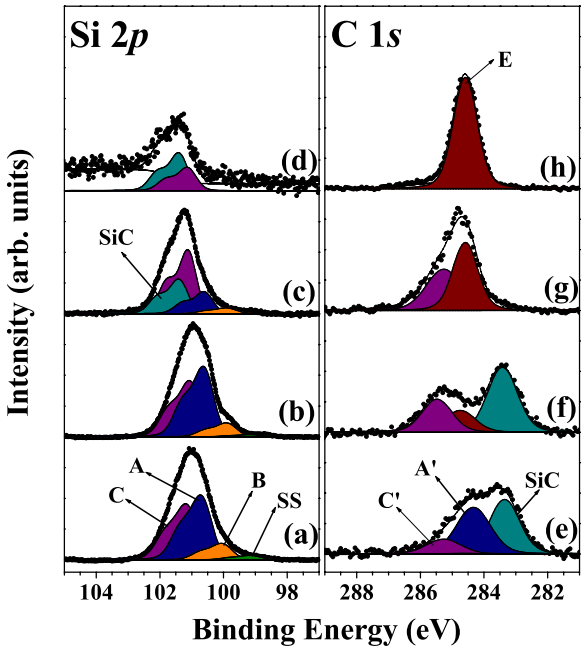

Figure 3. Photoemission spectra for the four different surface reconstructions. (a) and (e): annealed at 900 °C for 5 min with Si flux; (b) and (f): annealed at 1080 °C 5 min; (c) and (g): annealed at 1150 °C for 2 min; and (d) and (h): annealed at 1400 °C for 2 min. The binding energies of the peaks are SS: 99.2 eV, B: 100.1 eV, A: 100.7 eV, C: 101.2 eV, and SiC: 101.4 eV in Si 2p spectra, A′: 284.3 eV, C′: 285.3 eV, and SiC:283.3 eV, and E: 284.6 eV in C 1s spectra. The dots are experimental values and the solid lines represent the results of peak fitting.

where α and θ are the angle between the molecular axis and the surface normal and the angle between the light polarization vector (E-vector) and the surface normal, respectively, and P is the degree of polarization.

For this experiment, we assumed a polarization factor of $P = 0.85$ [27]. The ϕ^* resonance intensity is strong when the photon beam is incident with an angle of $\theta = 20°$ (glancing incidence), whereas it is weak when the incident photon angle is $\theta = 90°$ (normal incidence). We were able to calculate the tilting angle of the graphene sheet using the experimentally measured variation of the relative intensity for the 285.5 eV ϕ^* (C=C) resonance with the polarization vector angle. These values were obtained by measuring the height of the ϕ^* (C=C) resonance intensity. As a result of this quantitative analysis, the average angle obtained from these results is $14 \pm 2°$ on the reconstruction at 1150 °C. Similarly, the tilting angle on the 1×1 reconstruction after annealing at 1400 °C was found to be $7 \pm 2°$. Unfortunately, we were unable to calculate the angle value at 1080 °C because its phase is mixed, as explained in figure 1.

Near edge x-ray adsorption spectroscopy (NEXAFS) provides averaged values for the tilted angle C=C bonding of the graphene layers with respect to the SiC substrate. As a result, the graphene layers of the grains are tilted with respect to the surface. If the domain size of the tilted graphene layer is larger than the electron beam size (∼1 mm), the LEED spots are expected to be split. However, the domain size of the graphene layers grown on the SiC substrate was found to be smaller than the electron beam according to the atomic force microscopy (AFM) studies [14] and they were also likely to have ripples because of the lattice mismatch between the graphene layer and SiC substrate. We also confirmed from the spot profiles for the two samples (not shown here) that the full width at half maximum (FWHM) of the LEED peak for the 1150 °C sample is broader than that of the 1400 °C sample. Such broadening of the LEED spot may be attributed to the graphene layers consisting of smaller grains or similar grains with more wrinkled graphene layers compared to the 1400 °C sample surface. Therefore, low energy electron diffraction (LEED) results are in good agreement with the NEXAFS results.

Figure 3 displays the Si 2p (left panel) and C 1s (right panel) core level spectra obtained after annealing in the range from 900 to 1400 °C using a photon energy of 130 eV for Si 2p and 320 eV for C 1s to enhance the surface sensitivity. An important result provided by these surface sensitive core level spectra is that both Si and C atoms are present in the outermost layers for all three surface reconstructions. Moreover, the graphene thickness can be determined from the attenuation of the Si 2p peaks. A curve fitting procedure[4] was utilized in order to extract the shifts and relative intensities of the various

[4] Fitting program developed by Dr H D Kim in SNU (Pohang Accelerator laboratory, Korea).

components in the C 1s and Si 2p spectra for the reconstructed surfaces.

Figure 3(a) shows Si 2p core level spectrum obtained after annealing at 900 °C for 5 min during depositing of Si. Each spectrum was measured at the surface normal emission. As shown in this figure, we found four different Si 2p peaks of surface state (marked as SS), bulk state (marked as B), SiC induced peak (marked as A), and graphene induced peak (marked as C). Interestingly, we could observe the graphene induced peak (marked as C) at this annealing temperature although we did not see it in the LEED pattern. This means that the graphene layer exists at the subsurface. To monitor the changes among the four different bonding features as a function of the annealing temperature, we increased the annealing temperature. As the temperature increases up to 1080 °C for 5 min in figure 3(b), we could see that the silicon-rich layer is slightly increased. On the other hand, the surface state starts to diminish. Continuing at the annealing temperature of 1150 °C, we found that the surface state completely disappeared and the graphene layer is vividly increased, as shown in figure 3(c). This may be attributed to the fact that the graphene layer is dominant at this annealing temperature, which matches well with our LEED result. Finally, we increase the annealing temperature at 1400 °C to track the change in graphene layer. As shown in figure 3(d), the graphene layer is remarkably decreased and the SiC layer is dominant. Conclusively, we found that the graphene layer was formed at an annealing temperature of 1150 °C and it was dominant.

Concurrently, we also obtained C 1s core level spectra varying with the annealing temperature. The result of C 1s is the same as the trend of Si 2p. Figure 3(e) shows a C 1s core level spectrum obtained after annealing at 900 °C for 5 min after deposition of Si. As shown in this figure, it contains three components; two major components located at binding energies of 283.4 and 284.3 eV, which originate from SiC and $(\sqrt{3} \times \sqrt{3})$R30°, and a minor peak positioned at a binding energy of 285.3 eV, which originates from developing $(6\sqrt{3} \times 6\sqrt{3})$R30°. These finding led us to confirm also that the Si-rich reconstructed layer (marked as A′) and graphene induced layer (marked as C′) coexist at this annealing temperature. Increasing the annealing temperature up to 1080 °C, we also found an increment of the graphene layer shown in figure 3(f). The intensity of the 285.3 eV component increases as the $(6\sqrt{3} \times 6\sqrt{3})$R30° reconstruction becomes dominant. The original lower-lying structures located near 283.4 and 284.4 eV are considerably weaker after annealing at 1080 °C. At 1150 °C, we could see that the graphene layer is dominant, as shown in figure 3(g). After annealing at 1150 °C, two peaks are present at 285.3 and 284.6 eV because of the well-developed $(6\sqrt{3} \times 6\sqrt{3})$R30° and 1 × 1 reconstructions. Finally, when the annealing temperature was increased to around 1400 °C, there was only one feature at the binding energy of 284.6 eV. This means that the graphene layer has disappeared and a single phase graphite layer exists at this annealing temperature (marked as E).

The spectral analysis of Si 2p and C 1s core level spectra as a function of the annealing temperature revealed that the graphene layer is stably formed at the annealing temperature of 1150 °C.

Table 1. The values of angle and the expected thickness the graphene layer with varying annealing temperatures of (a) 1080 °C, (b) 1150 °C, and (c) 1400 °C, respectively.

$T_{\text{ann.}}$ (°C)	Structure	Angle (deg)	Expected thickness (Å)
1080	$(\sqrt{3} \times \sqrt{3})$R30° + $(6\sqrt{3} \times 6\sqrt{3})$R30°	N/A	3.2
1150	$(6\sqrt{3} \times 6\sqrt{3})$R30°	14 ± 2	6.6 ± 1
1400	1×1	7 ± 2	12 ± 1

In general, the attenuation of the Si 2p core level was determined by comparing the Si 2p signals measured before and after formation of the graphene layer with the expression [27].

$$d = \lambda \ln\left(\frac{I}{I_0}\right) \tag{2}$$

where I_0 and I are the Si 2p intensities before and after growth of the overlayer respectively.

The inelastic mean free path was assumed to be 3.2 Å at a photon energy of 130 eV [24]. The graphene layer thickness on the $(6\sqrt{3} \times 6\sqrt{3})$R30° reconstruction after annealing at 1150 °C was estimated to be around 6.6 ± 1 Å. This result is comparable to that found in the bilayer graphene in previous studies. The thickness was found to increase to 12 ± 1 Å on 1×1 reconstruction after annealing at 1400 °C. This result is comparable to four-layer graphene.

Table 1 summarizes the tilted angle and the expected thickness of graphene layer with varying annealing temperature.

4. Conclusion

The changes in the properties of graphene surfaces with variation in their growth conditions were measured using PES, LEED, and NEXAFS. We found that a bilayer-like thin graphene sheet is formed after annealing at 1150 °C. The tilting angle of the graphene sheet was estimated to be $14 \pm 2°$. As the thickness of the graphene layers increased, this angle gradually decreases to $7 \pm 2°$ at 1400 °C. Even though the graphene layers are moderately well grown on the SiC substrate with an almost flat lying geometry and good directionality, the measured tilt angle was bigger than expected because of the interface between graphene and SiC. The existence of the interface had more influence on thin layers than on thick layers.

Acknowledgments

This work was supported by a Korea Science and Engineering Foundation (KOSEF) grant funded by the Korean government (MOST) (No. 2007-01156) and the SRC program (Center for Nanotubes and nanostructured composites) of MOST/KOSEF, the Center of Fusion Technology for Security, the National R&D Projects for Nano Science and Technology Korea Research Grant No. KRF-2005-070-C00063, a Korea Research Foundation Grant funded by the Korean Government

(MOEHRD) (KRF-2006-311-C00307), and the experiments at PLS were supported in part by MOST and POSTECH.

References

[1] Geim A K and Novoselov K S 2007 *Nat. Mater.* **6** 183
[2] Wallace P R 1947 *Phys. Rev.* **71** 622
[3] Zhang Y B, Tan Y-W, Stormer H L and Kim Ph 2005 *Nature* **438** 201
[4] Novoselov K S, Geim A K, Morozov S V, Jiang D, Katsnelson M I, Grigorieva I V, Dubonos S V and Firsov A A 2005 *Nature* **438** 197
[5] Novoselov K S, Geim A K, Morozov S V, Jiang D, Zhang Y, Dubonos S V, Grigorieva I V and Firsov A A 2004 *Science* **306** 666
[6] Berger C, Song Z, Li T, Li X, Ogbazghi A Y, Feng R, Dai Z, Marchenkov A N, Conrad E H, First Ph N and de Heer W A 2004 *J. Phys. Chem.* B **108** 19912
[7] Bergerc, Song Z, Li X, Wu X, Brown N, Naud C, Mayou D, Li T, Hass J, Marchenkov 1 A N, Conrad E H, First Ph N and de Heer W A 2006 *Science* **312** 1191
[8] Meyer J C, Geim A G, Katsnelson M I, Novoselov K S, Booth T J and Roth S 2007 *Nature* **446** 60
[9] Wang S, Wang J, Miraldo P, Zhu M, Outlaw R, Hou K, Zhao X, Holloway B C and Manos D 2006 *Appl. Phys. Lett.* **89** 183103
[10] Heersche H B *et al* 2007 *Nature* **446** 54
[11] Stankovich D, Dikin D A, Dommett G H B, Kohlhaas K M, Zimney E J, Stach E A, Piner R D, Nguyen S T and Ruoff R S 2006 *Nature* **442** 282
[12] Johanson L I, Owman F and Martensson P 1996 *Phys. Rev.* **53** 13793
[13] Ohta T, Bostwick A, Seyller T, Horn K and Rotenberg E 2006 *Science* **313** 951
[14] Seyller Th, Emtsev K V, Gao K, Speck F, Ley L, Tadich A, Broekman L, Riley J D, Leckey R C G, Rader O, Varykhalov A and Shikin A M 2006 *Surf. Sci.* **600** 3906
[15] Forbeaux I, Themlin J-M, Charrier A, Thibaudau F and Debever J-M 2000 *Appl. Surf. Sci.* **162/163** 406
[16] Jikimoto T, Wang J L, Saito T, Hirai M, Kusaka M, Iwami M and Nakata T 1998 *Appl. Surf. Sci.* **130–132** 593
[17] Angot T, Portail M, Forbeaux I and Layet J M 2002 *Surf. Sci.* **502/503** 81
[18] Rollings E, Gweon G-H, Zhou S Y, Mun B S, McChesney J L, Hussain B S, Fedorov A V, First P N, de Heer W A and Lanzaraa A 2006 *J. Phys. Chem. Sol.* **67** 2172
[19] Johansson L I, Glans P-A and Hellgren N 1998 *Surf. Sci.* **405** 288–97
[20] Bostwick A, Ohta T, McChesney J L, Emtsev K V, Seyller T, Horn K and Rotenberg E 2007 *New J. Phys.* **9** 385
[21] Ohta T, El Gabaly F, Bostwick A, McChesney J L, Emtsev K V, Schmid A K, Seyller T, Horn K and Rotenberg E 2008 *New J. Phys.* **10** 023034
[22] Mallet P, Varchon F, Naud C, Magaud L, Berger C and Veuillen1 J-Y 2007 *Phys. Rev.* B **76** 041403(R)
[23] Kaplan R 1989 *Surf. Sci.* **215** 111
[24] Himpsel F J, McFeely F R, T-Ibrahimi A and Yarmoff J A 1988 *Phys. Rev.* B **38** 6084
[25] Stöhr J 1992 *NEXAFS Spectroscopy* (New York: Springer)
[26] Stöhr J and Outka D A 1987 *Phys. Rev.* B **36** 7891
[27] Krinsky S, perlman M L and Watson R E 1983 *Hand Book on Synchrotron Radiation* ed E E Koch (Amsterdam: North-Holland)